We are IntechOpen,
the world's leading publisher of
Open Access books
Built by scientists, for scientists

4,800
Open access books available

122,000
International authors and editors

135M
Downloads

154
Countries delivered to

Our authors are among the

TOP 1%
most cited scientists

12.2%
Contributors from top 500 universities

CLARIVATE ANALYTICS
BOOK CITATION INDEX
INDEXED

WEB OF SCIENCE™

Selection of our books indexed in the Book Citation Index
in Web of Science™ Core Collection (BKCI)

Interested in publishing with us?
Contact book.department@intechopen.com

Structural and Electronic Properties of Graphene upon Molecular Adsorption: DFT Comparative Analysis

Ali Zain Alzahrani
Physics Department, Faculty of Science,
King Abdulaziz University
Saudi Arabia

1. Introduction

Since its discovery in 2004 (Nobel prize in 2010), graphene -a single sheet of carbon atoms forming the thinnest free standing material to date- has attracted enormous interest due to its potentially tunable and exotic structural and electronic properties (Castro Neto et al., 2009; Geim & Novolselov, 2007; Katsnelson et al., 2006, 2007; Novoselov et al., 2004, 2007; Ohta et al., 2006; Y. Zhang et al., 2005). The pristine graphene is characterized as a zero-gap semiconductor with bonding π and antibonding π^* bands touch in a single point at the Fermi level (E_F) at the corner of the Brillouin zone, and close to this so-called Dirac point the bands display a linear dispersion, leading to extremely high charge carriers mobility at room temperature of approximately 15,000 cm^2/V.s (Geim & Novolselov, 2007) which is significantly higher than that of the widely-used semiconductor, *namely* silicon (Si), of approximately 1400 cm^2/V.s. Like carbon nanotubes, measurements (Lee et al., 2008) have shown that graphene is extremely strong and rigid compared to Si-based materials. These incredibly fascinating properties alongside the high thermal conductivity suggest that graphene is an excellent candidate for the applications in the circuits beyond the conventional complementary metal-oxide semiconductor technology and many other potential applications. Moreover and recently, the possibility of using graphene as a highly-sensitive gas sensor has been reported as the good sensor properties of carbon nanotubes are already known. It was shown that the increase of the concentration of graphene charge carrier induced by adsorbed gas molecules can be used to make highly sensitive sensors. These highly-sensitive properties of graphene can be attributed to the fact that graphene is a low-dimensional structure with only a surface but no volume which increase the chemical reaction of adsorbates and the surface atoms. Additionally, the high conductivity of graphene even in low charge density is another reason for being a highly-sensitive sensor.

Having established the importance of pristine graphene in many potential applications, the adsorption of single atoms (Chan et al., 2008; Farjam & Rafii-Tabar, 2009; Han et al., 2007; Hao et al., 2006; Li et al., 2008; Mao et al., 2008; Medeiros, 2010; Yang, 2009) and molecules (Duplock et al., 2004; Elias et al., 2009; Giannozzi et al., 2003; Ito et al., 2008; Leenaerts et al., 2008, 2009; Nakamura et al., 2008; Novoselov et al., 2004; Pinto et al., 2009; Sanyal et al.,

2009; Schedin et al., 2007; Wehling et al., 2008; Y.-H. Zhang, 2010) on the bare graphene surface has been the subject for different theoretical and experimental investigations due to their promising applications in nanoscale electronics, bioelectronics, gas sensors, and hydrogen storage devices. Among these adsorbates, hydrogen has been considered as one of the most interesting and fantastic candidates. Recently, it has been experimentally reported, using the transmission electron microscopy, that a graphene sheet can be chemically converted into graphane through a hydrogenation process by reacting with atomic hydrogen (Elias et al., 2009). This process, however, transforms the zero-gap semiconductor graphene into a wide-gap semiconductor (insulator) graphane. Theoretically reported studies (Boukhvalov et al., 2008; Sofo et al., 2007) using the density functional scheme, have revealed that the chairlike configuration, with hydrogen atoms attached to the carbon atoms in alternative manner, is the energetically most preferable structure for graphane. Sofo *et al.* (Sofo et al., 2007) have found that the chairlike and boatlike conformers are semiconducting with 3.5 eV and 3.7 eV, respectively. As has been claimed in many literatures (H. Ohno, 1998; Y. Ohno et al., 1999; Savchenko, 2009), future hydrogen-fuel technologies should make use of graphane as hydrogen storage due to its very high hydrogen density. Moreover, this extremely thin material with a finite band gap is also likely to find its use in many technological and industrial applications. Overall, graphene surface could be successfully used as a base for creating new promising and useful materials, and it would be of quite interest to theoretically investigate the effects of incorporating various molecules into its structure for different technological and industrial applications.

The adsorption of various molecules onto graphene has also been investigated. The structural and electronic properties of oxygen-adsorbed graphene have been theoretically studied by Nakamura *et al.* (Nakamura et al., 2008) and Ito *et al* (Ito et al., 2008). Their results have indicated that the adsorption of oxygen molecules onto graphene produces epoxy and ether group phases which are almost bistable. Moreover, they have concluded that the ether structure is the most energetically preferable for adsorption involving both sides of the sheet, while the one-side adsorption structure appears only as a meta-stable phase, with a finite energy gap at the K point emerges and its value increases as the number of oxygen increases with respect to the number of carbon atoms. The key charge transfer mechanisms upon adsorption of NH_3, NO, and NO_2 onto graphene have been reported by Leenaerts *et a*l. (Leenaerts et al., 2008, 2009). Their theoretical results indicate that the NO_2 adsorbates induce a relatively strong doping comparing to the NO molecule. Within the framework of the local density approximation of the density functional theory, Pinto *et al.* (Pinto et al., 2009) have investigated the chemisorption of tetrafluoro-tetracyanoquinodimethane (F4-TCNQ) molecule on pristine graphene by means of the electronic properties. It was reported that the F4-TCNQ molecule acts like a p-type dopant for graphene with an approximately charge of 0.3 e/molecule being transferred from the highest occupied molecular orbital (HOMO) of graphene to the lowest unoccupied molecular orbital (LUMO) of the molecule. Zhang *et al.* (Y.-H. Zhang et al., 2010) have recently investigated the binding of organic electron donor and acceptor molecules on graphene sheets within the framework of the density functional theory. They found that the adsorption of 2,3-dichloro-5,6-dicyano-1,4-benzoquinone (DDQ) and tetrathiafulvalene (TTF) cause hybridizations between the molecular levels and the graphene valence bands. These hybridizations transform the zero-gap semiconductor graphene into a metallic graphene. Despite the available studies, there are no enough theoretical comparative study

on the physics and chemistry of the adsorption of small molecules onto the surface of pristine graphene.

In the present chapter, we aim to theoretically investigate the fundamental changes of the structural and electronic properties of graphene upon the incorporation of hydrogen, benzene, and naphthalene molecules. The first-principles calculations will be performed using the density functional theory in its local density approximation scheme and the pseudopotential method.

2. Calculation methodology

The present *ab initio* calculations have been performed using the density functional theory (DFT) (Hohenberg & Kohn, 1964) with a plane wave basis set as implemented in the QUANTUM ESPRESSO simulation package (Giannozzi et al., 2009). The electron–electron interactions were expressed within the local density approximation (LDA) as parameterized by Perdew and Zunger (Perdew & Zunger, 1981). The electron–ion interaction was treated by using the ultrasoft pseudopotential for carbon and hydrogen (Vanderbilt, 1990). We expanded the single-particle Kohn–Sham (Kohn & Sham, 1965) wave functions using a linear combination of plane-wave basis sets with a kinetic energy cutoff of 45 Ry. The Kohn–Sham equations were Self consistently solved by employing a 14×14×1 **k** points Monkhorst–Pack set (Monkhorst & Pack, 1976) within the hexagonal Brillouin zone. The repeated supercell technique was used to model the studied graphene-based structures. In each surface structure of pristine and molecule-adsorbed graphene we considered a 6×6×1 unit cell containing 72 carbon atoms. We have used our calculated in-plane lattice parameter for graphene of 2.45 Å which is in good agreement with the previously reported theoretical (Ito et al., 2008; Schabel & Martins, 1992; Yin & Cohen, 1984) and experimental values for bulk graphite (D. Mckie & C. Mckie, 1986). To minimize the interactions between the graphene sheet and its periodic image, we considered a vertical separation of 14.65 Å (six times the lattice parameter) along the surface normal direction. These parameters have been carefully chosen after several calculations to obtain well-converged results. Relaxed atomic positions for carbon and hydrogen atoms were obtained by using the total-energy and force minimization methods following the Hellmann–Feynman approach. The equilibrium atomic positions were determined by relaxing all atoms in the cell except the carbon atom at the origin which was kept in its bulk position.

3. Results and discussion

In the following subsections we will present, based on *ab initio* calculations, a comparative study of the structural and electronic properties of pristine graphene, hydrogen-adsorbed graphene (graphane), benzene-adsorbed graphene, and naphthalene-adsorbed graphene. To establish well-defined comparative study we have performed the calculations using unit cells of similar sizes and parameters.

3.1 Pristine graphene

It is rather important for our present comparative study to start with the structural and electronic properties of the pristine graphene. Figure 1 shows a schematic view of the fully-relaxed structure of the pristine graphene, indicating the basic structural parameters. It is well-known that each carbon atom has two 2*s* and two 2*p* electrons in its valence

state. These four electrons lead to various *sp*-hybridized orbitals. For graphene, each carbon atom is bonded to three other carbon atoms according to an *sp*^{2} hybridization. In the present calculations the C-C bonds are found to be 1.41 Å which are smaller than the C-C bond lengths of diamond of 1.52 Å. The C-C-C angle is measured to be 120° which is slightly larger than the prospective value of 109.5° in its diamond structure. These values suggest that, unlike the ideal *sp*^{3} diamond structural phase, graphene has a significant *sp*^{2} nature as stated above. This feature, therefore, leads to the considerable rigidity of graphene materials comparing with the normal semiconducting materials, such as Si.

The electronic band structure of the clean graphene sheet is plotted in Fig. 2 along the principal directions of the hexagonal Brillouin zone. It is clearly shown that the band structure of pristine graphene has a zero-gap semiconducting nature. It is important to note the folding of the bands due to the used supercell. In this plot, the top of the valence state and the bottom of the conduction state degenerate at the Γ point (Dirac point) instead of the K point of the hexagonal Brillouin zone. These two bands obey a linear in-plane dispersion relation near the Fermi energy at the Γ point of the Brillouin zone resulting in zero effective mass for electrons and holes and high mobility of charge carriers.
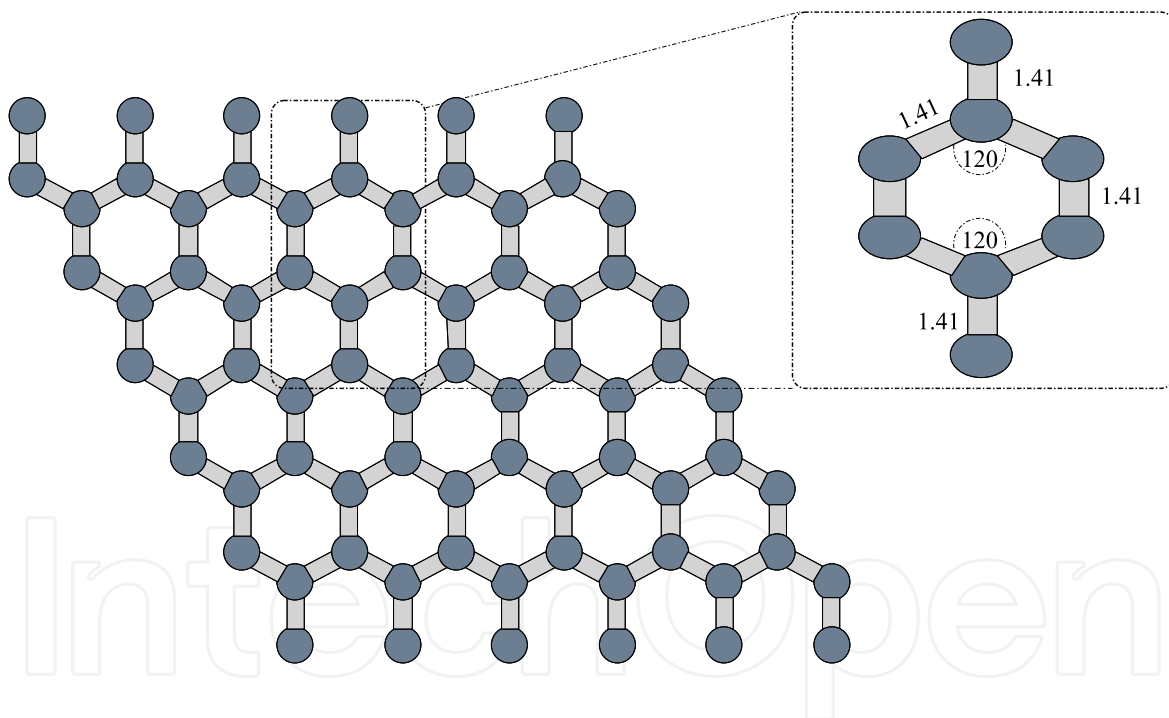

Fig. 1. Schematic top view of the optimized structure of pristine graphene. The inset shows the structural parameters of the hexagonal ring. The bond lengths are measured in angstrom (Å) and angles are measured in angles (°).

In a previous report (AlZahrani & Srivastava, 2009) we have studied the in-plane dispersion curves, at the Γ point, slightly above and slightly below the Fermi energy to extract the velocities of electron and hole carriers. These velocities were estimated to be 1.11×10⁶ m/s and 1.04×10⁶ m/s. The partial charge density plots of these two states at the K point confirm the bonding π and antibonding π* orbital nature of the HOMO and LUMO states of pristine graphene, as clearly shown in Fig. 3.
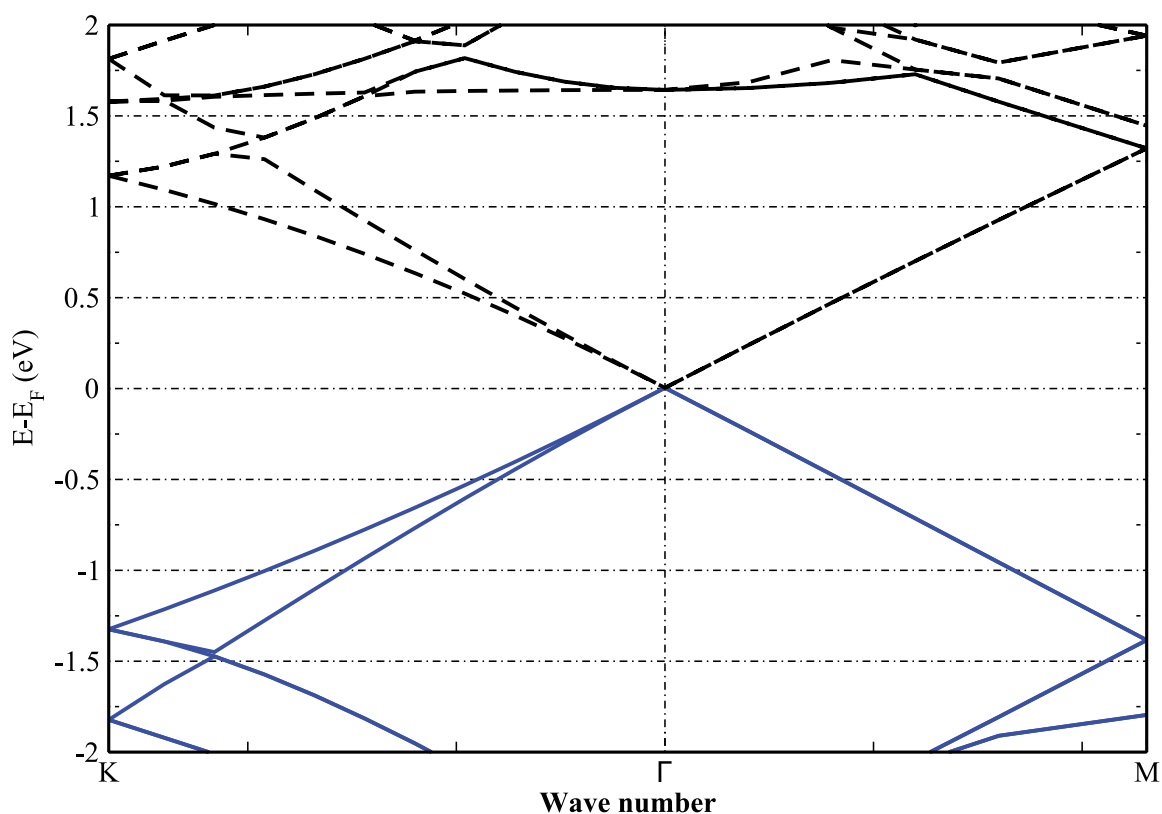
Fig. 2. Electronic band structure of the pristine graphene along the principal directions of the hexagonal Brillouin zone. The Fermi level is set at the zero.
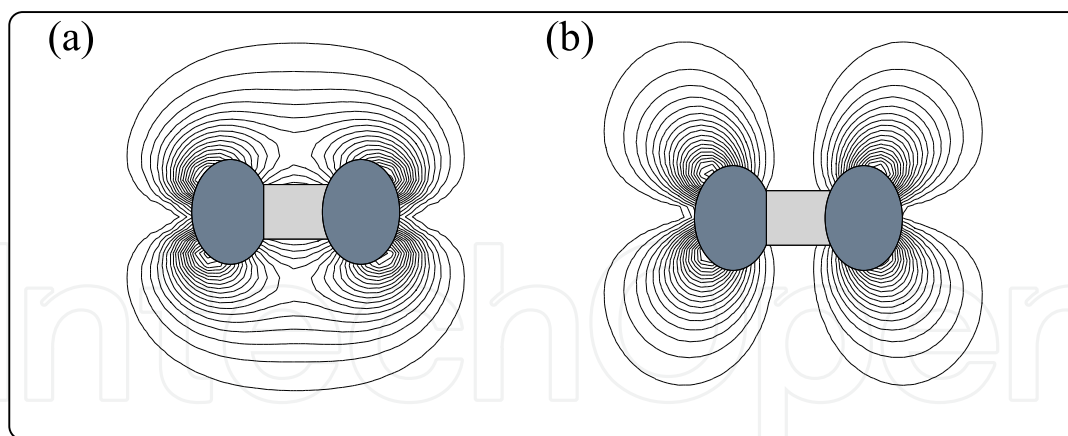

Fig. 3. Partial charge density plot, at the K point, of the (a) highest occupied state and (b) lowest unoccupied state.

3.2 Hydrogen-adsorbed graphene

The chemical adsorption of hydrogen atoms on pristine graphene has gained great interest due to the immense changes in the electronic properties of graphene. These changes lead to a new wide-gap semiconducting material which has the name of *graphane*. Subsequently, graphane has been experimentally synthesized and reported that it obeys a reversible hydrogenation-dehydrogenation process (Elias et al., 2009). This material, therefore, could

open the gate for enormous technological and industrial applications, such as hydrogenstorage and two-dimensional nanoelectronics. Our purpose in this section is to find the energetically most stable geometry of graphane and then to compare its structural and electronic properties with those of pristine graphene. To model such a material, we have initially considered four different preliminary configurations depending on the adsorption sites of hydrogen atoms above and/or below the graphene sheet. These structures are chairlike, boatlike (Sofo et al., 2007), tablelike, and stirrup configurations as schematically shown in Fig. 4. The key building block of these structures is the number and orientation (up or down) of the attached hydrogen atoms in each hexagonal cell of graphene. The chairlike conformer consists of hydrogen atoms which are alternatively attached to the carbon atoms on both sides of the sheet. The hydrogen atoms in the boatlike conformer are alternatively attached in pairs to the carbon atoms on both sides. In the tablelike configuration the hydrogen atoms are attached to every carbon atom from one side of the sheet. Finally, the stirrup structure has three hydrogen atoms attached to the carbon atoms from the upper side of the sheet and also three others attached to the carbon atoms from the bottom side. Our self-consistent calculations indicate that the chairlike configuration is the energetically most stable structure (minimum energy structure) with an energy gain of approximately 0.129 eV, 0.131 eV, and 0.655 eV comparing with the boatlike, stirrup, and tablelike configurations,
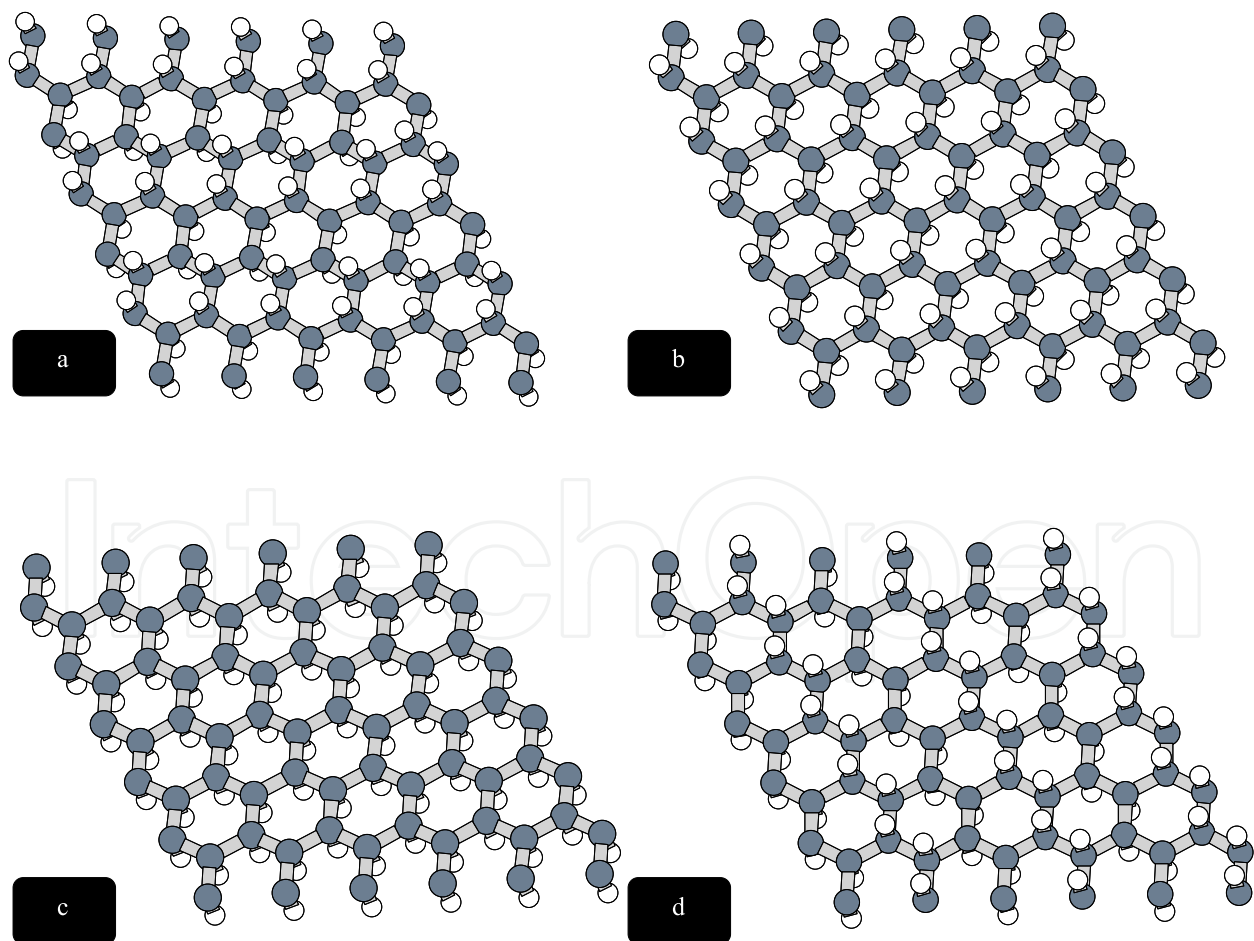

Fig. 4. Schematic view of the optimized structures of the possible structures of hydrogen-adsorbed graphene (graphane) with (a) boatlike, (b) chairlike, (c) tablelike, and (d) stirrup.

respectively. These findings for chair and boatlike structures are very comparable with the previously reported results obtained by Sofo *et al.* (Sofo et al., 2007). We note that boatlike and stirrup configurations are almost meta-stable structures and can be found in H-rich environment. In the following lines, we will focus our discussion on the structural and electronic properties of the ground state structure of graphane (chairlike conformer).

We have started our calculations for chairlike geometry of graphane with a flat sheet of graphene and hydrogen atoms at 1.0 Å above carbon species. Minimization of this structure leads to a fully-relaxed configuration as schematically depicted in Fig. 5. From this figure we have found that the C–C bond length is approximately 1.49 Å, which is larger than the C–C bond length in the ideal graphene (1.42 Å). However, this value is almost comparable with the C–C bond length obtained for graphite (1.47 Å) and diamond (1.52 Å) using similar computational parameters. Moreover, the calculated graphane C–C bond length is in excellent agreement with the bond length of 1.48 Å obtained by Igami *et al.* (Igami et al. 2001). Upon the H adsorption, the basis carbon atoms in the cell are found to experience a vertical buckling (perpendicular distance between the two carbon sublattices) of approximately 0.46 Å, which is in excellent agreement with the theoretical values obtained by Boukhvalov *et al.* (Boukhvalov et al., 2008) and Sahin *et al.* (Sahin et al., 2010) and the experimental value extracted by Elias *et al* (Elias et al., 2009). Having this amount of buckling, the lattice constant of graphene increases from 2.45 Å to 2.50 Å. This amount of buckling leads not only to a structural variation but also to a significant change in the electronic properties of graphene.
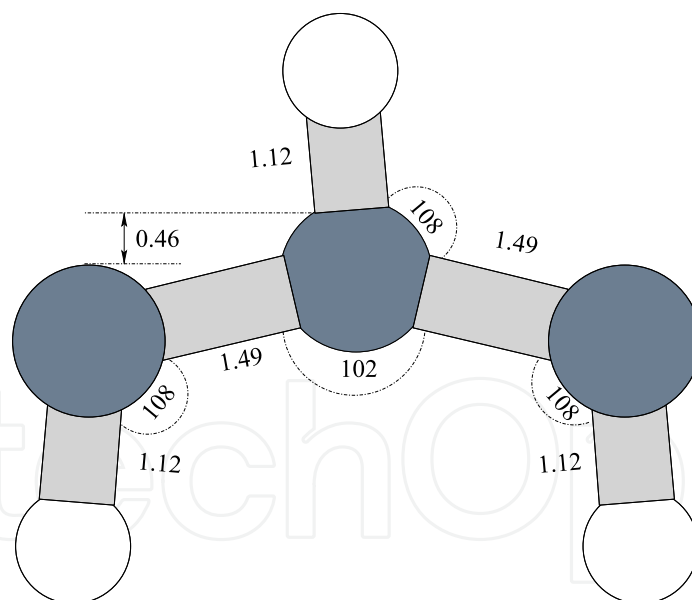

Fig. 5. The optimized atomic structure of the chairlike configuration along with the key-structural parameters. The bond lengths and angles are measured angstrom and degrees, respectively.

Consistent with previously reported results (Boukhvalov et al., 2008; Sahin et al., 2010; Sofo et al., 2007), the C–H bond length is measured to be 1.12 Å, which is identical to the typical bond length of the hydrocarbon compounds. While the angle between two adjacent C-C bonds (C-C-C angle) is found to be 102°, the angle between C-H and C-C bonds (C-C-H angle) is determined to be 108°. The average value of these angles is slightly smaller than

the tetrahedral angle of diamond of 109.5°. These values are in mild agreement with the previous theoretical results (Boukhvalov et al., 2008; Sahin et al., 2010). However, this suggests that the nature of C–C and C–H bonds is not entirely sp^3 but sp^3-like. Overall, these findings for calculated bond lengths and angles clearly indicate that the bonding in graphane is sp^3-like.
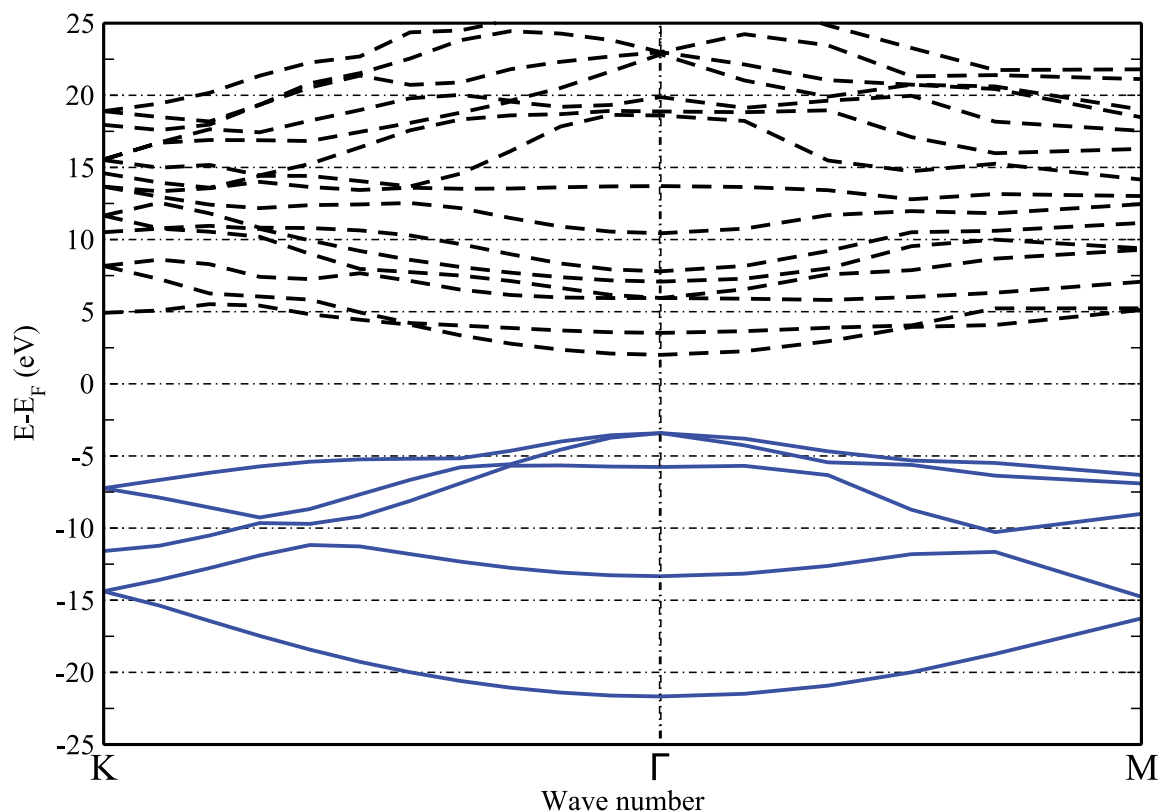

Fig. 6. Surface electronic band structure of the most stable structure of graphane (chairlike) along the principal directions of the hexagonal Brillouin zone. The Fermi level is set at the zero.

The electronic band structure of chairlike graphane is calculated along the principal directions of the hexagonal Brillouin zone as shown in Fig. 6. It is clearly noted that the bonding π and antibonding π^* states of clean graphene are now removed. Since graphane is an sp^3-like saturated structure with every C atoms being bounded to three adjacent C atoms and a single H atom, the system is found to be non-magnetic semiconducting with a direct LDA band gap of 3.9 eV, with HOMO at E_F -3.4 eV and LUMO at E_F +2.5 eV.

This value of band gap is slightly larger than the reported value of 3.5 eV (Sofo et al., 2007). It is rather important to indicate that due to the well-known deficiency of the LDA in dealing with semiconducting systems, the underestimated band gap of 3.9 eV is corrected by GW_0 approximation to become 5.97 eV (Lebèrgue et al., 2009). From Fig. 6, we clearly note that the uppermost occupied band is doubly degenerate at approximately 7 eV below the Fermi level at the zone edge, *namely* K point. This degeneracy has also been observed for pristine graphene but with energetic shift due to the charge transfer from H atoms towards the graphene. We also find a double degeneracy of the top of valence band at about 3 eV below the Fermi level. Such degeneracy suggests that these bands have a symmetrical

orbital nature but with different effective masses. Above the Fermi level, we can identify band degeneracy at the zone edges K and M with eigenvalues of 8 eV and 5 eV, respectively. These features can be directly related to the graphene sheet as we have noted in Fig. 2 but with significant change in their energies. Inspection of the partial charge density, at the K point, of both HOMO and LUMO states reveals that the π bonding orbital in C-C bonds of graphene is broken and a new sp_z orbital is created between H and the upper C atom (i.e. the carbon atom that was tilted upwards) upon hydrogenation process. Moreover, the antibonding π* orbital in graphene is removed and replaced by the antibonding state which is a hybridization of the H s and C p orbitals. These plots are shown in Fig. 7.
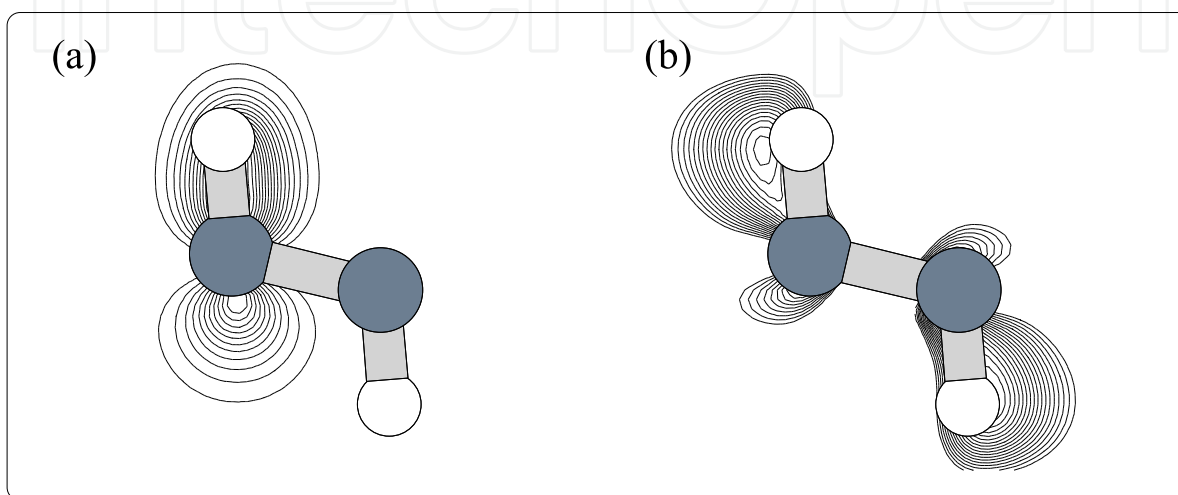

Fig. 7. Partial charge density plot, at the K point, of the (a) highest occupied state and (b) lowest unoccupied state of chairlike graphane.

It is quite important for the device engineering and manufacturing to figure out the bonding nature of C-C and C-H bonds. To perform such an examination, we performed total charge density calculations in a plane and along the C–C and C–H bonds. Figure 8(a) shows a contour map of the total charge density in [010]/[001] plane. It clearly indicates that the charge distribution around the C-C bond is supportive of that in tetrahedrally coordinated diamond as shown in Fig. 8(b). Our results indicate that the C–C and C–H bonds have a noticeable degree of covalency, as shown in panels (c) and (d) of Fig. 8. A considerable amount of charge is uniformly localized around the carbon atoms. It is interesting to note that the double-hump feature of the charge density along the neighboring C atoms (Fig. 8(c)) is typical of the diamond structure, which is not an artifact of the pseudopotential method. Moreover, we have clearly observed that a little amount of charge being transferred from the hydrogen towards the carbon atoms. Quantitatively, we have used the Löwdin population analysis scheme (Lowdin, 1950) to obtain numeral information about the atomic charges. Employing this scheme, the wave functions are projected onto linear combinations of atomic orbitals; we find that a charge of 0.2e has been transferred from the hydrogen atoms to the carbon atoms for each unit cell. Our calculated value is in good match with the result obtained by Sofo et al (Sofo et al., 2007).

3.3 Benzene-adsorbed graphene

Rather than hydrogen, it has been reported that the adsorption of organic molecules on graphene leads to significant changes in the fundamental atomic and electronic properties of the substrate. To examine the reliability of these changes we will study the mechanism of

the chemisorption of small molecules (benzene and naphthalene) on a clean sheet of graphene. This subsection will be designed to study the benzene-adsorbed graphene structure whereas the next subsection will detail the naphthalene-adsorbed graphene system. To investigate the basic properties of graphene upon the adsorption of benzene, we firstly check different possible adsorption sites of the molecule onto the substrate.
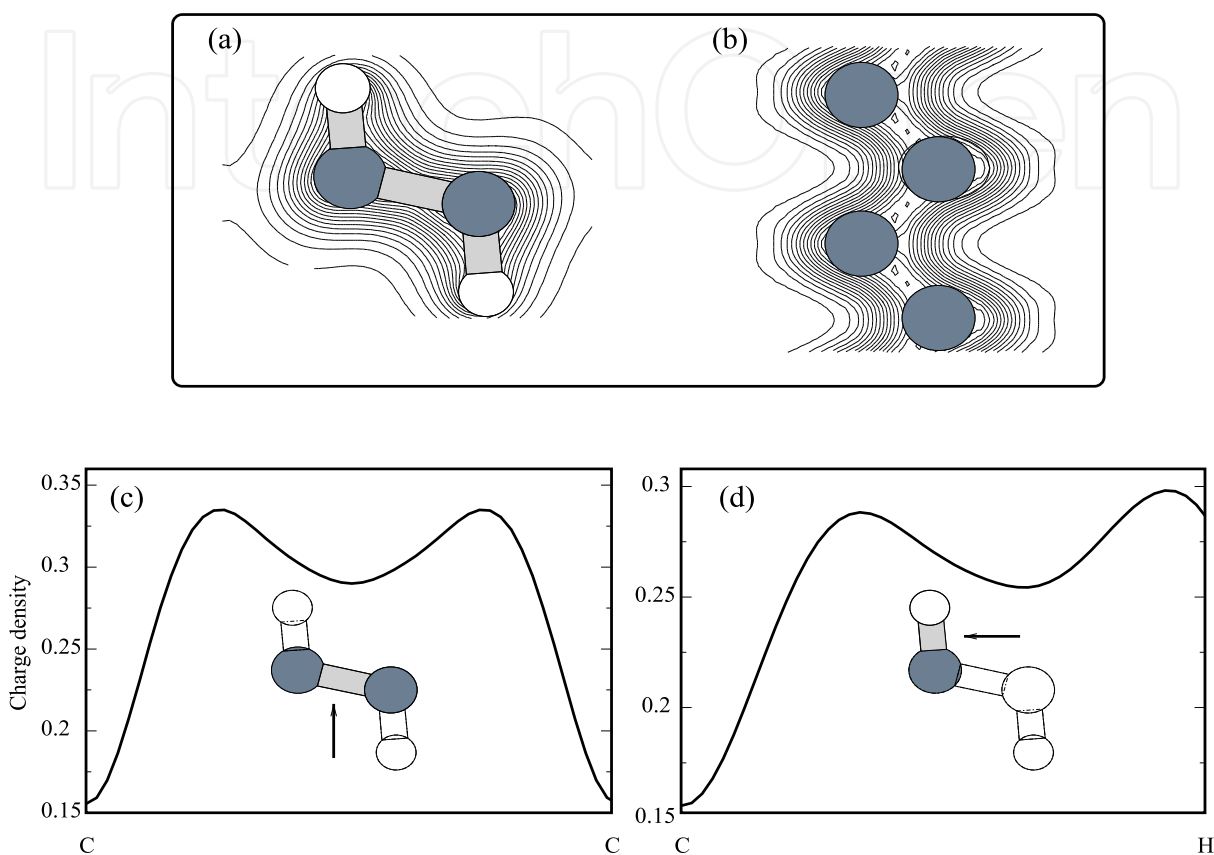

Fig. 8. Total charge density contour plots of (a) graphane and (b) diamond in a plane passing though H-C-C-H and C-C-C-C lines, respectively. Total charge density plot along the (c) C-C and (d) C-H bonds in graphane. The charge density is measured in e/a.u^3.

Neglecting the unfavorable substitutional sites, we have considered two configurations for the adsorption of benzene on pristine graphene. In these we have attempted a hollow and a stack adsorption sites, as schematically shown in Fig. 9. Therefore, to evaluate the energetically most preferable configuration between them, we compare their surface formation energies according to the formula:

$$\Delta E = E_{BG} - E_G - E_B. \tag{1}$$

The symbols E_{BG}, E_G and E_B indicate the total energies of the optimized structures of the benzene-adsorbed graphene, pristine graphene, and isolated benzene molecule, respectively. It is important to state that these total energies are calculated within similar unit cells and computational parameters. Using the above equation we find that the adsorption energies of hollow and stack structures are approximately -0.25 eV and -0.30 eV, respectively. These values suggest that the stack configuration represent the ground-state structure of the benzene-graphene system with energy gain of about 0.05 eV comparing with the hollow

phase. Therefore we will focus our theoretical investigation on the stack configuration to determine the structural and electronic properties of benzene/graphene structure. The starting point towards the structural optimization of the present system is the initial position of benzene molecule above the graphene sheet. The molecular atoms (benzene molecule) are initially placed at 1.5 Å above the carbon atoms of the graphene. After several iterations of relaxation process, the benzene molecule adopts a planar geometry at 3.52 Å above the graphene sheet. While this value is consistent with the experimental value of 3.6 Å that is estimated from binding energy curves performed by Chakarova-Kack *et al.* (Chakarova-Kack et al., 2006), it is slightly larger than the value of 3.17 Å obtained by Zhang *et al* (Y.-H. Zhang et al., 2010). This inconsistency is due to the quite low energy cutoff used in their calculations. Subsequently we have found that the C–C and C–H bond lengths of benzene on the top of graphene are measured to be 1.39 Å and 1.10 Å, respectively. These values are identical to those of the hydrocarbons compounds of 1.40 Å and 1.10 Å for C-C and C-H bonds, respectively. Since the calculated C–C–C and C–C–H angles of the molecule are identical and equal to 120°, we conclude that benzene reorients itself in a planar manner above the graphene. This orientation has also been noted for F4-TCNQ (Pinto et al., 2009) which indicates similar adsorption mechanism for organic molecules on graphene. Adsorbed-graphene sheet, on the other side, has been found to have a C–C bond length of 1.41 Å and a C–C–C angle of 120°. These suggest that, even though benzene is being adsorbed, graphene preserves its basic structural behaviour.
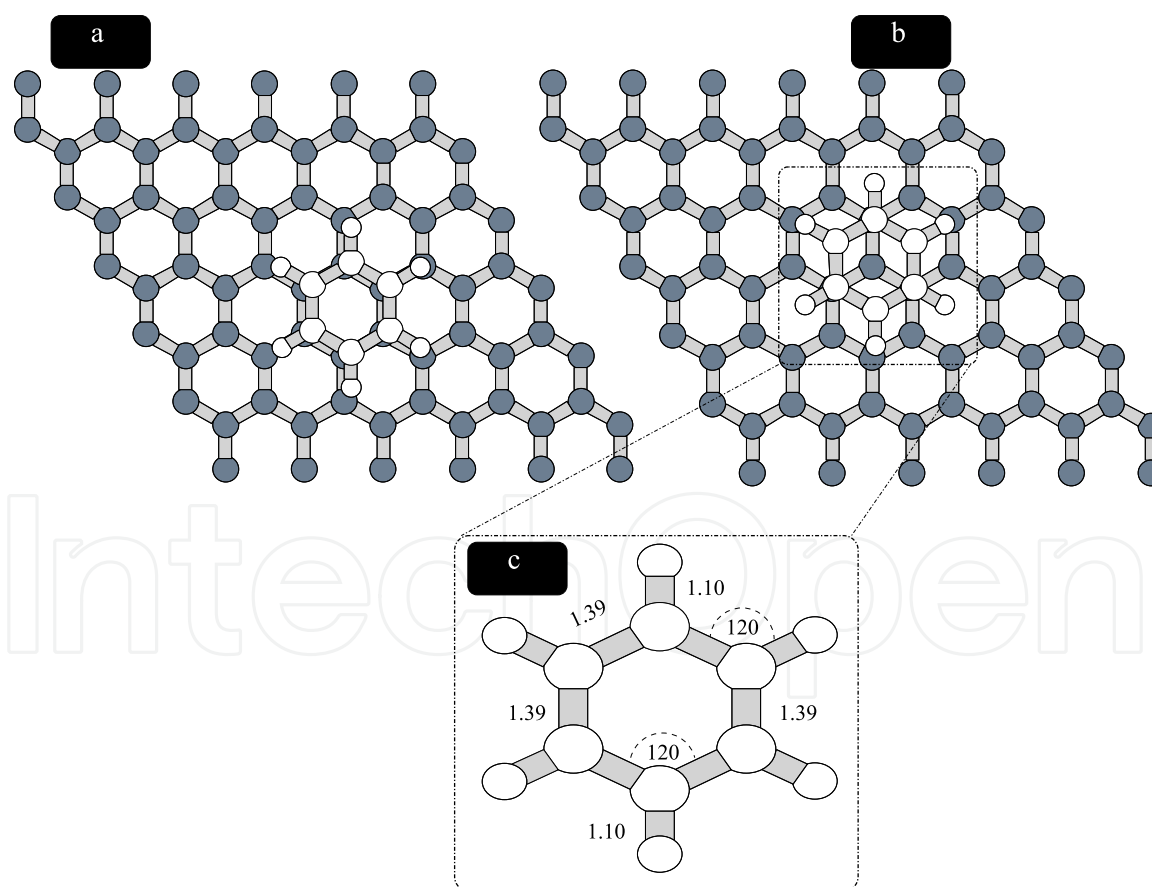

Fig. 9. Schematic view of the minimum-energy structures of the (a) hollow and (b) stack configurations of benzene-adsorbed graphene. (c) Top view of the relaxed benzene molecule with its structural parameters. The grey solid spheres represent C atoms from the graphene while dashed spheres indicate C atoms from the molecule.

Further, we have performed surface electronic band structure for the benzene-adsorbed graphene configuration along the high-symmetry directions, K→Γ and Γ→M, as shown in Fig. 10. Setting the Fermi level at the zero-energetic position, we clearly note that the Dirac point of the systems is coincided with the Fermi level, indicating a zero-gap nature. This indicates that, for low-energy states, the adsorption of benzene leads to unchanged electronic structure regarding to pristine graphene. Accordingly, this suggests that charge transfer is not expected to occur between the graphene and the molecule. Such an observation can be understood if we believe that only the states very far below/above the Dirac point of graphene are perturbed by the molecular adsorption. However, this conclusion is supportive of the result obtained by Zhang *et al*. (Y.-H. Zhang et al., 2010). In their study they found that the adsorption of benzene on pristine graphene results in insignificant amount of electronic charge being transferred from the molecule to the graphene sheet.
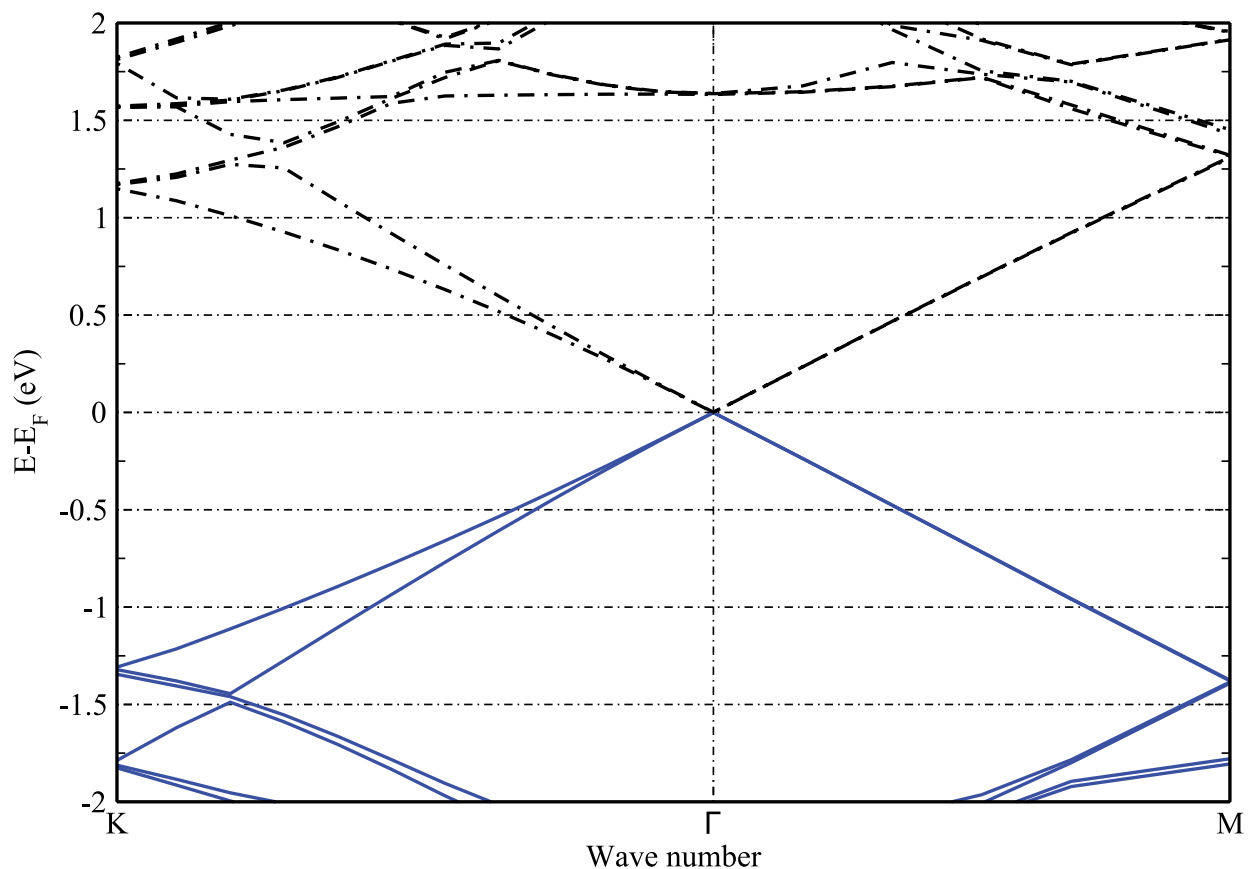

Fig. 10. Electronic band structure of the benzene-adsorbed graphene system with the molecule on a stack adsorption site. The zero-energy position indicates the Fermi level.

3.4 Naphthalene-adsorbed graphene

As has been performed for benzene-adsorbed graphene structure, we have tested at least two adsorption sites for naphthalene molecule onto graphene. Between hollow and stack configurations we have found that the latter represents the minimum-energy structure of naphthalene-adsorbed graphene, as shown in Fig. 11. Our calculations indicates that the adsorption energy of stack and hollow phases are approximately −0.47 eV and −0.39 eV,

respectively. The molecule is found to be relaxed 3.15 Å above the sheet suggesting no bond formation between the molecule fragments and the carbon atoms of the graphene. Looking at the C–H bond length of the molecule we have identified no appreciable change and its typical value of 1.10 Å. Comparing the naphthalene-adsorbed system with the benzene-adsorbed system, we have clearly noted considerable alterations in the C–C bond lengths of the molecule. These bond lengths are categorized into three groups: 1.37 Å, 1.40 Å, and 1.43 Å. These values are in the acceptable range of the typical bond lengths of an isolated naphthalene molecule (1.36–1.42 Å). The C–C–C and C–C–H angles vary in the interval 121–122° and 118–120°, respectively. These results suggest a very tiny amount of vertical tilt in the carbon planes. However, the substrate keeps its original structure as also seen for benzene-adsorbed structure.
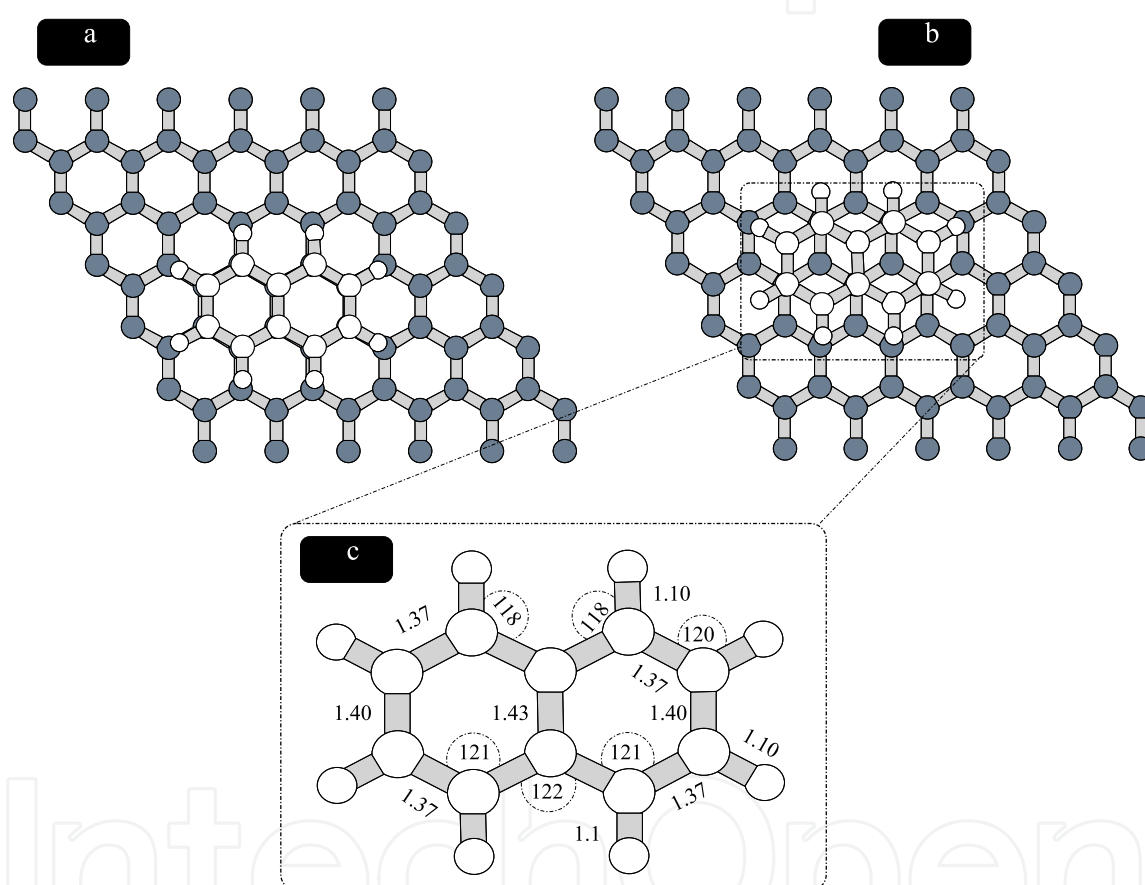

Fig. 11. The minimum-energy structures of the (a) hollow and (b) stack configurations of naphthalene-adsorbed graphene. (c) Top view of the fully relaxed molecule.

In Fig. 12, we have depicted the electronic band structure of the naphthalene/graphene system. Despite that the band structure for the benzene/graphene system looks very similar to the pristine graphene in the low-energy region (±2.0 eV with respect to Fermi level E_F), the energy bands for the naphthalene/graphene system performs little changes below the Fermi level. From the figure we clearly identify a new flat (non-dispersive) band at energy of E_F −1.3 eV. This band is believed to be originated from the molecule states. Overall, the system has an entire zero-gap behaviour with indication that no charge being transferred from/to the graphene substrate.
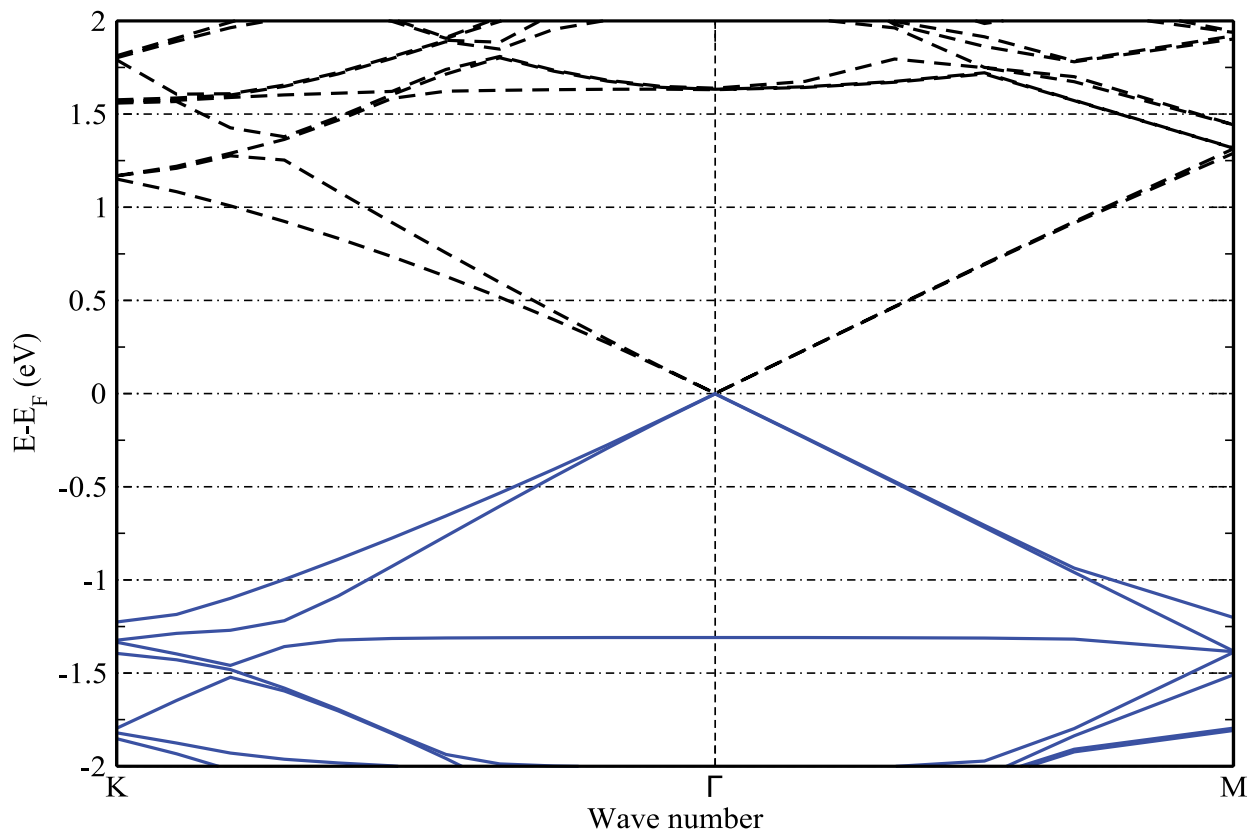
Fig. 12. Electronic band structure of the naphthalene/graphene system with the molecule on a stack adsorption site. The Fermi level is located at the zero-energy position.

4. Conclusion

Within the framework of local density approximation of the density functional theory and pseudopotential theory we have presented a comparative *ab initio* study for the adsorption of molecules on a pristine graphene. The *sp²* structure and zero-gap behaviour are found to the fundamental characteristics of clean graphene with degenerate bonding π and antibonding π^* states at the K point. Upon the adsorption of hydrogen atoms on pristine graphene, a chairlike configuration is found to be the energetically most stable structure for the system (graphane). As the four valence electrons of carbon atoms participate in the formation of the covalent bonzds with hydrogen atoms the π bands are removed from the band structure of graphane. The absence of these bands leads graphane to be a semiconducting with wide direct gap at the Γ point. Moreover, the structural transformation of carbon bonds from *sp²* to *sp³*-like hybridization results in an increase in the bond length from 1.41 Å to 1.49 Å. Unlike the hydrogen-adsorbed graphene, benzene and naphthalene-adsorbed structures are found to only stabilize the graphene sheet with no significant change in its low-energy electronic properties.

5. References

AlZahrani, A. Z. & Srivastava, G. P (2009). Gradual changes in electronic properties from graphene to graphite: first-principles calculations. *Journal of Physics: Condensed Matter* Vol. 21, No. 49, (November 2009), pp. 495503- 495509, ISSN 0953-8984

Boukhvalov, D. W.; Katsnelson, M. I. & Lichtenstein, A. I. (2008). Hydrogen on graphene: Electronic structure, total energy, structural distortions and magnetism from first-principles calculations. *Physical Review B* Vol. 77, No. 3, (January 2008), pp. 035427-035433, ISSN 1098-0121

Castro Neto, A.H.; Guinea, F.; Peres, N.M.R.; Novoselov, K.S. & Geim, A.K. (2009). The electronic properties of graphene. *Reviews of Modern Physics* Vol. 81, No. 1, (January 2009), pp. 109-162, ISSN 0034-6861

Chakarova-Kack, S.D.; Schroder, E.; Lundqvist, B. & Langreth, D. (2006). Application of van der Waals Density Functional to an Extended System: Adsorption of Benzene and Naphthalene on Graphite. *Physical Review Letters* Vol. 96, No. 14, (April 2006), pp. 146107-146110, ISSN 0031-9007

Chan, K. T.; Neaton, J. B. & Cohen, M. L. (2008). First-principles study of metal adatom adsorption on graphene. *Physical Review B* Vol. 77, No. 23, (June 2008), pp. 235430-235441, ISSN 1098-0121

Duplock, E.J.; Scheffler, M. & Lindan, P.J.D. (2004). Hallmark of Perfect Graphene. *Physical Review Letters* Vol. 92, No. 22, (June 2004), pp. 225502-225505, ISSN 0031-9007

Elias, D.C.; Nair, R. R.; Mohiuddin, T. M. G.; Morozov, S. V.; Blake, P.; Halsall, M. P.; Ferrari, A. C.; Boukhvalov, D. W.; Katsnelson, M. I.; Geim, A. K. & Novoselov, K. S. (2009). Control of Graphene's Properties by Reversible Hydrogenation: Evidence for Graphane. *Science* Vol. 323, No. 5914, (January 2009), pp. 610-613, ISSN 0036-8075

Farjam, M. & Rafii-Tabar, H. (2009). Energy gap opening in submonolayer lithium on graphene: Local density functional and tight-binding calculations. *Physical Review B* Vol. 79, No. 4, (January 2009), pp. 045417-045423, ISSN 1098-0121

Geim, A. K. & Novoselov, K. S. (2007). The rise of graphene. *Nature Materials* Vol. 6, (March 2007), pp. 183 - 191 ISSN 1476-1122

Giannozzi, P.; Car, R. & Scoles, G. (2003). Oxygen adsorption on graphite and nanotubes. *The Journal of Chemical Physics* Vol. 118, No. 3, (November 2002), pp. 1003-1006, ISSN 0021-9606

Giannozzi, P.; Baroni, S.; Bonini, N.; Calandra, M.; Car, R.; Cavazzoni, C.; Ceresoli, D.; Chiarotti, G.L.; Cococcioni, M.; Dabo, I.; Dal Corso, A.; de Gironcoli, S.; Fabris, S.; Fratesi, G.; Gebauer, R.; Gerstmann, U.; Gougoussis, C.; Kokalj, A.; Lazzeri, M.; Martin-Samos, L.; Marzari, N.; Mauri, F.; Mazzarello, R.; Paolini, S.; Pasquarello, A.; Paulatto, L.; Sbraccia, C.; Scandolo, S.; Sclauzero, G.; Seitsonen, A.P.; Smogunov, A.; Umari, P. & Wentzcovitch, R.M. (2009). *Journal of Physics: Condensed Matter* Vol. 21, No. 39, (September 2009), pp. 395502- 395520, ISSN 0953-8984

Han, M. Y.; Özylmaz, B.; Zhang, Y. & Kim, P. (2007). Energy Band-Gap Engineering of Graphene Nanoribbons. *Physical Review Letters* Vol. 98, No. 20, (May 2007), pp. 206805-206808, ISSN 0031-9007

Hao, S. G.; Zhou, G.; Duan, W. H.; Wu, J. & Gu, B. L. (2006). Tremendous Spin-Splitting Effects in Open Boron Nitride Nanotubes: Application to Nanoscale Spintronic Devices. *Journal of the American Chemical Society* Vol. 128, No. 26, (June 2006), pp. 8453-8458, ISSN 0002-786

Hohenberg, P. & Kohn, W. (1964). Inhomogeneous Electron Gas. *Physical Review* Vol. 136, No. 3B, (November 1964), pp. B864-B871, ISSN 0031-899X

Igami, M.; Okada, S. & Nakada, K. (2001). Electronic and geometric structures of fluorine adsorbed graphene. Synthetic Metals Vol. 121, No. 1-3, (March 2001), pp. 1233-1234, ISSN 0379-6779

Ito, J.; Nakamura, J. & Natori, A. (2008). Semiconducting nature of the oxygen-adsorbed graphene sheet. *Journal of Applied Physics* Vol. 103, No. 11, (June 2008), pp. 113712-113716, ISSN 0021-8979

Katsnelson, M. I.; Novoselov, K. S. & Geim, A. K. (2006). Chiral tunnelling and the Klein paradox in graphene. *Nature Physics* Vol. 2, (September 2006), pp. 620-625, ISSN 1745-2473

Katsnelson, M. I. (2007). Graphene: carbon in two dimensions. *Materials today* Vol. 10, No. 1-2, (January-February 2007), pp. 20-27, ISSN 1369-7021

Kohn, W. & Sham, L. (1065). Self-Consistent Equations Including Exchange and Correlation Effects. *Physical Review* Vol. 140, No. 4A, (November 1965), pp. A1133–A1138, ISSN 0031-899X

Lebègue, S.; Klintenberg, M.; Eriksson, O. & Katsnelson, M. I. (2009). Accurate electronic band gap of pure and functionalized graphane from GW calculations. *Physical Review B* Vol. 79, No. 24, (June 2009), pp. 245117 -245121, ISSN 1098-0121

Lee, C.; Wei, X.; Kysar, J. W. & Hone, J. (2008). Measurement of the Elastic Properties and Intrinsic Strength of Monolayer Graphene. *Science* Vol. 321, No. 5887, (July 2008), pp. 385-388, ISSN 0036-8075

Leenaerts, O.; Partoens, B. & Peeters, F.M. (2008). Adsorption of H_2O, NH_3, CO, NO_2, and NO on graphene: A first-principles study. *Physical Review B* Vol. 77, No. 12, (March 2008), pp. 125416-125421, ISSN 1098-0121

Leenaerts, O.; Partoens, B. & Peeters, F.M. (2009). Adsorption of small molecules on graphene. *Microelectronics Journal* Vol. 40, No. 4-5, (April-May 2009), pp. 860-862, ISSN 0026-2692

Li, X.; Wang, X.; Zhang, L.; Lee, S. & Dai, H. (2008). Chemically Derived, Ultrasmooth Graphene Nanoribbon Semiconductors, *Science* Vol. 319, No. 5867, (February 2008), pp. 1229-1232, ISSN 0036-8075

Löwdin, P. O. (1950). On the Non-Orthogonality Problem Connected with the Use of Atomic Wave Functions in the Theory of Molecules and Crystals. Journal of Chemical Physics Vol. 18, No. 3, (March 1950), pp. 365-375, ISSN 0021-9606

Mao, Y.; Yuan, J. & Zhong, J. (2008). Density functional calculation of transition metal adatom adsorption on graphene. *Journal of Physics: Condensed Matter* Vol. 20, No. 11, (February 2008), pp. 115209-115214, ISSN 0953-8984

McKie, D. & McKie, C. (1986). *Essentials of Crystallography*, Blackwell Science, 978-0632015740 Oxford, United Kingdom

Medeiros, P.V.C.; Mota, F.; Mascarenhas, A.J.S. & Castilho, C.M. (2010). A DFT study of halogen atoms adsorbed on graphene layers. *Nanotechnology* Vol. 21, No. 48, (November 2010), pp. 115701-115708, ISSN 0957-4484

Monkhorst, H.J. & Pack, J.D. (1976). Special points for Brillouin-zone integrations. *Physical Review B* Vol. 13, No. 12, (June 1976), pp. 5188–5192, ISSN 1098-0121

Nakamura, J.; Ito, J. & Natori, A. (2008). Structural bistability of the oxygen-adsorbed graphene sheet. *Journal of Physics: Conference Series* Vol. 100, Part 5, (May 2008), pp. 052019-052022, ISSN 1742-6588

Novoselov, K. S.; Geim, A. K.; Morozov, S. V.; Jiang, D.; Zhang, Y.; Dubonos, S. V. & Firsov, A. A. (2004). Electric Field Effect in Atomically Thin Carbon Films. *Science,* Vol. 306, No. 5696, (October 2004), pp. 666-669, ISSN 0036-8075

Novoselov, K. S.; Jiang, Z.; Zhang, Y.; Morozov, S. V.; Stormer, H. L.; Zeitler, U.; Maan, J. C.; Boebinger, G. S.; Kim, P. & Geim, A. K. (2007). Room-Temperature Quantum Hall Effect in Graphene. *Science* Vol. 315, No. 5817, (March 2007), pp. 1379, ISSN 0036-8075

Ohno, H. (1998). Making Nonmagnetic Semiconductors Ferromagnetic. *Science* Vol. 281, No. 5379, (August 1998), pp. 951-956, ISSN 0036-8075

Ohno, Y.; Young, D. K.; Beschoten, B.; Matsukura, F.; Ohno, H. & Awschalom, D. D. (1999). Electrical spin injection in a ferromagnetic semiconductor heterostructure. *Nature* Vol. 402, (December 1999), pp. 790-792, ISSN: 0028-0836

Ohta, T.; Bostwick, A.; Seyller, T.; Horn, K. & Rotenberg, E. (2006). Controlling the Electronic Structure of Bilayer Graphene. *Science* Vol. 313, No. 5789, (August 2006), pp. 951-954, ISSN 0036-8075

Pinto, H.; Jones, R.; Goss, J.P. & Briddon, P.R. (2009). p-type doping of graphene with F4-TCNQ. *Journal of Physics: Condensed Matter* Vol. 21, No. 40, (September 2009), pp. 402001-402003, ISSN 0953-8984

Perdew, J. P. & Zunger, A. (1981). Self-interaction correction to density-functional approximations for many-electron systems. *Physical Review B* Vol. 23, No. 10, (May 1981), pp. 5048–5079, ISSN 1098-0121

Şahin, H.; Ataca, C. & Ciraci, S. (2010). Electronic and magnetic properties of graphane nanoribbons. *Physical Review B* Vol. 81, No. 20, (May 2010), pp. 205417-205424, ISSN 1098-0121

Sanyal, B.; Eriksson, O.; Jansson, U. & Grennberg, H. (2009). Molecular adsorption in graphene with divacancy defects. *Physical Review B* Vol. 79, No. 11, (March 2009), pp. 113409-113412, ISSN 1098-0121

Savchenko, A. (2009). Tranforming Graphene. *Science* Vol. 323, No. 5914, (January 2008), pp. 589-590, ISSN 0036-8075

Schabel, M.C. & Martins, J.L. (1992). Energetics of interplanar binding in graphite. *Physical Review B* Vol. 29, No. 11, (September 1992), pp. 7185–7188, ISSN 1098-0121

Schedin, F.; Geim, A.K.; Morozov, S.V.; Hill, E.W.; Blake, P.; Katsnelson, M.I. & Novoselov, K.S. (2007). Detection of individual gas molecules adsorbed on graphene. Nature Materials *Vol. 6,* (July 2007), pp. *652-655,* ISSN 1476-1122

Sofo, J. O.; Chaudhari, A. S. & Barber, G. B. (2007). Graphane: A two-dimensional hydrocarbon. *Physical Review B* Vol. 75, No. 15, (April 2007), pp. 153401-153404, ISSN 1098-0121

Vanderbilt, D. (1990). Soft self-consistent pseudopotentials in a generalized eigenvalue formalism. *Physical Review B* Vol. 41, No. 11, (April 1990), pp. 7892–7895, ISSN 1098-0121

Wehling, T.O.; Lichtenstein, A.I. & Katsnelson, M.I. (2008). First-principles studies of water adsorption on graphene: The role of the substrate. *Applied Physics Letters* Vol. 93, No. 20, (November 2008), pp. 202110-12, ISSN 0003-6951

Yang, C-K. (2009). A metallic graphene layer adsorbed with lithium. *Applied Physics Letters* Vol. 94, No. 16, (April 2009), pp. 163115-163117, ISSN 0003-6951

Yin, M.T. & Cohen, M. L. (1984). Structural theory of graphite and graphitic silicon. *Physical Review B* Vol. 29, No. 12, (June 1984), pp. 6996–6998, ISSN 1098-0121

Zhang, Y.; Tan, Y.; Stormer, H. & Kim, P. (2005). Experimental observation of the quantum Hall effect and Berry's phase in graphene. *Nature* Vol. 438, (November 2005), pp. 201-204 ISSN, 0028-0836

Zhang, Y.-H.; Zhou, K.-G.; Xie, K.-F.; Zeng, J.; Zhang, H.-L. & Peng, Y. (2010). Tuning the electronic structure and transport properties of graphene by noncovalent functionalization: effects of organic donor, acceptor and metal atoms. *Nanotechnology* Vol. 21, No. 6, (January 2010), pp. 065201-065207, ISSN 0957-4484
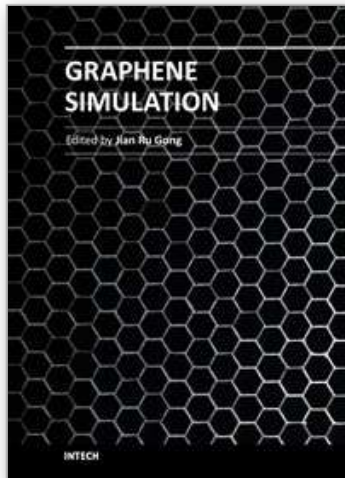
Graphene Simulation

Edited by Prof. Jian Gong

Graphene, a conceptually new class of materials in condensed-matter physics, has been the interest of many theoretical studies due to the extraordinary thermal, mechanical and electrical properties for a long time. This book is a collection of the recent theoretical work on graphene from many experts, and will help readers to have a thorough and deep understanding in this fast developing field.

How to reference

In order to correctly reference this scholarly work, feel free to copy and paste the following:

INTECH
open science | open minds